JOURNAL OF THE CAMEROON ACADEMY OF SCIENCES Vol. 8 No.1 (2008)

Petrology of spinel lherzolite xenoliths in alkali basalts from Liri, South of the Kapsiki Plateau (Northernmost Cameroon Hot Line)

NGOUNOUNO I.[1], NGUIHDAMA Dagwai[1], KAMGANG P.[2], DERUELLE B.[3]

[1]1Département des Sciences de la Terre, Faculté des Sciences, Université de Ngaoundéré B.P. 454, Ngaoundéré, Cameroun. ngounouno@yahoo.fr

[2]Département des Sciences de la Terre, Faculté des Sciences, Université de Yaoundé I B.P. 812, Yaoundé, Cameroun.

[3]Laboratoire de Magmatologie et Géochimie Inorganique et Expérimentale, Institut de Physique du Globe de Paris, UMR 1754, Université Pierre et Marie Curie, 4, place Jussieu, 75252 Cedex 05, France

RESUME

Des xénolites de lherzolite à spinelle, composés d'olivine (Fo_{88-91}), d'orthopyroxène (En_{89-91}), de clinopyroxène (6,5 % d'Al_2O_3) et du spinelle riche Al sont présents dans les basaltes alcalins de Liri, Sud du plateau Kapsiki, extrême nord de la "Ligne chaude du Cameroun". Les données pétrographiques sont présentées et les analyses à la microsonde électronique des phases minérales coexistant dans six xénolites de lherzolite à spinelle sont reportées, avec les analyses des phases minérales des basaltes-hôtes. Des réactions d'échange et de transfert régies par des lois thermodynamiques sont examinées ; elles ont permis de conclure que les lherzolites à spinelle de Liri montrent une homogénéité chimique interne et qu'elles représentent un manteau supérieur normal. Leurs compositions minéralogiques suggèrent des conditions d'équilibre de 1050-1200°C et 1,4-2,3 GPa.

Mots clés : xénolites, ultramafique, lherzolite, Liri, Ligne Chaude du Cameroun, pétrologie.

ABSTRACT

Spinel lherzolite xenoliths, composed of olivine (Fo_{88-91}), orthopyroxene (En_{89-91}), clinopyroxene (5.0 % Al_2O_3), and Al-rich spinel occur in alkali basalts from Liri, South of the Kapsiki plateau, northernmost Cameroon Hot Line. Petrographic data are given and microprobe analyses of coexisting phases in these spinel lherzolite xenoliths are reported, along with the analyses of host-basalts. Exchange and transfer reactions rules based on thermodynamic equilibrium conditions are examined. The Liri spinel lherzolites show internal chemical homogeneity and represented a normal upper mantle. Their mineral chemistries suggest equilibrium conditions of 1050-1200°C and 1.4-2.3 GPa.

Key words: xenoliths, ultramafic, lherzolite, Liri, Cameroon Hot Line, petrology.

INTRODUCTION

The Liri region, South of the Kapsiki Plateau, belongs to the Cameroon Hot Line (Déruelle et al., 2007; Fig. 1), an active N30°E tectono-magmatic alignment, extending from Pagalu Island to Lake Chad. Its oceanic sector is comprised of six major volcanoes, and the continental sector of seven major volcanoes, numerous monogenic cones and more than sixty plutonic anorogenic ring complexes. The Kapsiki Plateau is the northernmost volcanic zone of the Cameroon Hot Line. The volcanism (27-35 Ma) is of alkaline type and has typical bimodal lava series diversity with basalts and hawaiite as mafic lavas and phonolites and trachytes, and rhyolites as felsic lavas (Ngounouno et al., 2000).

Ultramafic xenoliths described here were sampled in basaltic lava flows of the monogenic cone North-West of Liri, and were first mentioned by Tamen (1998). Numerous occurrences of ultramafic xenoliths have been found in basaltic lavas all along the Cameroon Hot Line (Fig. 1) : six sites at Sao Tomé (Caldeira and Munha, 2002), two at Santa Isabel (Bioko) (Déruelle et al., 1991), and one in each of the other sites: Mt Cameroon (Ngounouno and Déruelle, 2007), Barombi-Mbo (Kumba) (Teitchou et al., 2007), Lake Enep (Oku) (Lee et al., 1996; Princivalle et al., 2000), and Nyos (Wum) (Nana et al., 1998). The rocks are mostly spinel lherzolites; some pyroxenites occur at Sao Tomé and Mt Cameroon. Spinel (Girod et al., 1984) and garnet (Temdjim, 2005) lherzolites are also present in the Adamawa. The purpose of the present study is to describe the petrography and composition of ultramafic xenoliths from Liri in order to determine their origin and their equilibrium conditions.

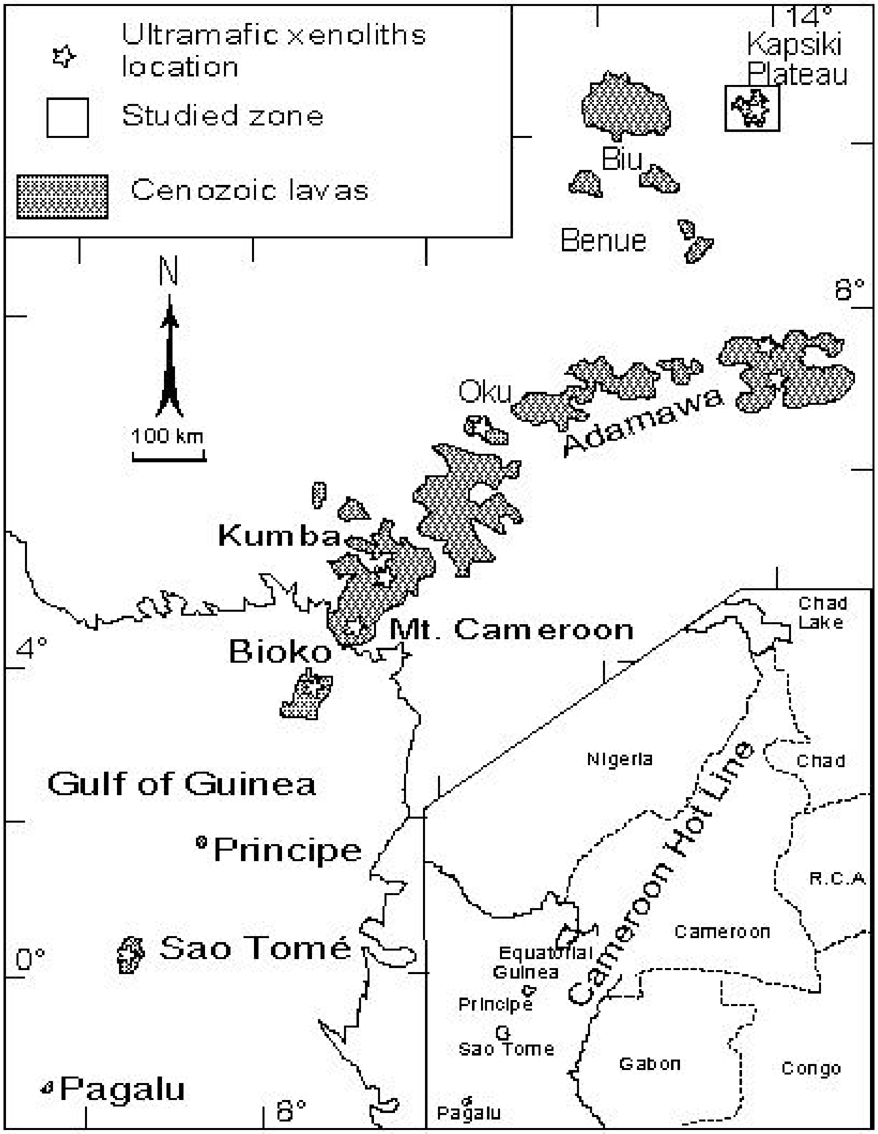

Fig. 1: Location of ultramafic xenoliths along the Cameroon Hot Line.

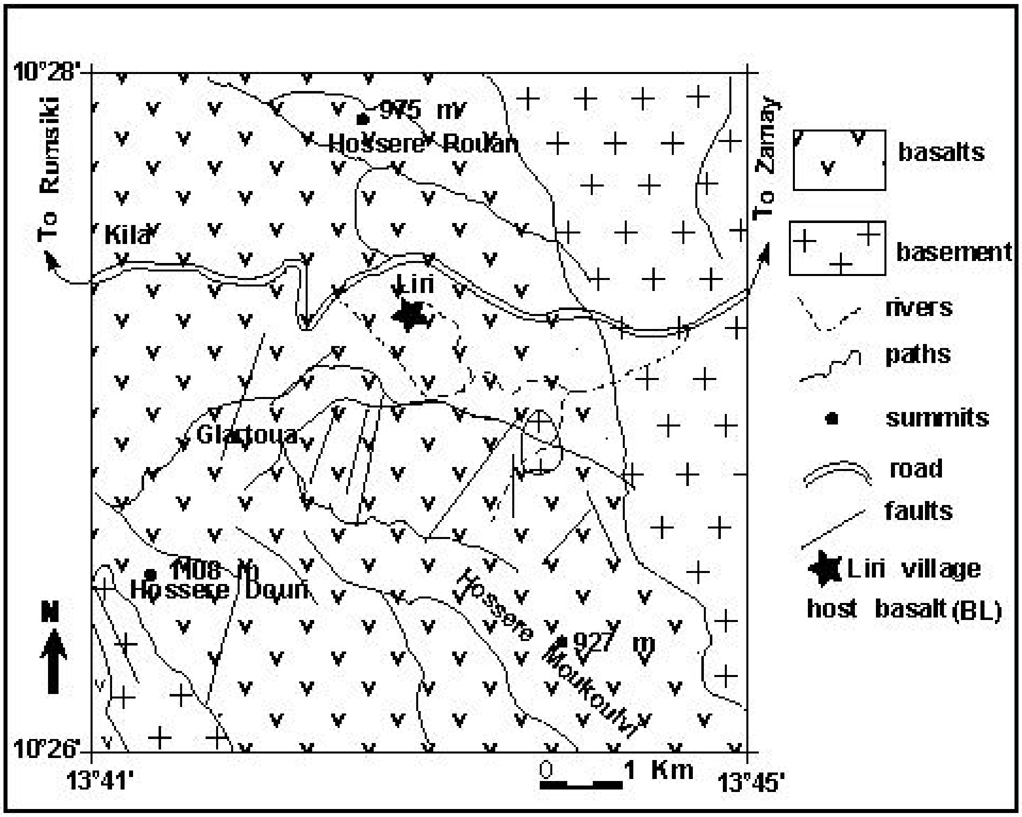

Fig. 2: Geological map of the Liri region and location of the spinel lherzolite xenoliths.

2. GEOLOGICAL SETTING AND SAMPLES LOCATION

The volcanism of the Liri region (Dumort and Péronne, 1966) is alkaline (Tamen, 1998) and characterized by a few small basaltic lava flows (Figure 2) intruded along the N65°E, N30°E and N165°E fractures (Moreau et al., 1986) of the Precambrian basement (Regnoult and Déruelle, 1983). The ages of these basalts are not precisely known. Nevertheless, similar basalts samples 15 km northwards in the Kapsiki Plateau gave K-Ar ages between 27.4 ± 0.5 Ma and 33.21 ± 1.33 Ma (Dunlop, 1983). The host rock (BL) represents basaltic lava flows and contains numerous spinel lherzolite xenoliths with sub-rounded shapes (7 to 30 centimetres in diameter).

3. ANALYTICAL METHODS

Mineral analyses reported here (Table 1) were made with the "Microscan 5" electro-probe microanalyser, Titanomagnetite (53 < Usp % < 62) ……..10-10 ($\pm 0.5 \times 10^{-10}$) and at the CAMPARIS analytical centre, Université Pierre et Marie Curie, Paris, on either a Cameca CAMEBAX or SX-50 microprobe, using the wavelength dispersive method. Pure elements, oxides, simple silicate compositions or sulphides were used as standards. Corrections were made for dead-time, atomic number, absorption and fluorescence using computer programes based on the methods of "PAP" (Pouchou and Pichoir, 1991). The analytical conditions (by element) are : olivine: 15 kV, 40 nA, 20 s, except Si: 10 s; orthopyroxene and clinopyroxene : 15 kV, 40 nA, 20 s, except Ti: 30 s (Fe^{3+} recalculated after Droop, 1987), Fe-Ti oxides: 20 kV, 40 nA, 40 s except Al and Cr: 30 s (Fe^{3+} recalculated after Stormer, 1983); plagioclase: 15 kV, 10 nA, 10 s ; spinel: 10 kV, 80 nA, 40 s except Al and Cr : 30 s, and Zn and Ni: 15 s. For pyroxenes, the nomenclature used is that of Morimoto et al. (1988). For spinel, Fe^{3+} is calculated by stoichiometry.

Major elements (Table 2) of the host basalt (BL) were made by inductively coupled plasma emission (ICP). Trace elements, including rare earth elements, were analyzed by inductively coupled plasma emission mass spectrometry (ICP-MS) at the Centre de Recherches Pétrographiques et Géochimiques (CRPG), Nancy, France. A full description of the techniques used, including analytical conditions and precision estimates, is given in Carignan et al. (2001).

Table 1: Chemical compositions of representative host-basalt from Liri (BL). The Mount Cameroon (C10J) and Kapsiki Plateau (52X) host-basalts are used in comparison.

rock	lherzolite								host-basalt						
mineral	ol		opx		cpx		sp		ol (ph)	ol (xeno)	opx	cpx	ilm	mt	plag
SiO_2 (wt %)	39.73	40.53	54.81	55.92	48.50	49.05			38.66	40.72	55.99	47.85	0.02	0.01	50.89
TiO_2			0.01	0.06	0.18	0.25	0.07	0.07			0.10	2.35	51.57	19.09	
Al_2O_3			2.38	3.04	4.44	4.93	50.53	52.49			3.16	6.59	0.07	2.85	30.89
Cr_2O_3	0.03	0.03	0.58	0.23	0.78	0.92	15.01	14.54		0.05	0.26		0.19	1.28	
FeO*	10.10	9.31	5.47	6.13	2.91	2.67	12.59	12.75	14.69	8.94	5.98	9.38	40.56	68.37	0.57
MnO	0.20	0.14	0.15	0.21	0.11	0.01	0.09	0.11	0.26	0.13	0.18	0.29	0.83	0.57	
MgO	48.94	49.26	34.68	33.02	20.87	19.50	19.58	19.51	45.12	49.06	33.06	11.22	5.44	3.17	
CaO	0.12	0.11	0.80	0.39	20.99	21.21	0.01	0.00	0.12	0.13	54.00	21.41	0.23	0.03	13.87
Na_2O			0.12	0.11	1.07	1.02	0.01	0.00				0.96			3.31
K_2O															0.12
NiO	0.40	0.31	0.12	0.11	0.03	0.08	0.35	0.29	0.35	0.41	0.13		0.11	0.00	
Total	99.55	99.71	99.12	99.22	99.87	99.64	97.89	99.76	99.20	99.43	99.53	99.38	99.02	95.37	99.66
FeO recalc.			1.83	6.13	1.47	1.58	9.376	10.12				5.95	35.47	43.27	0.57
Fe_2O_3 recalc.			4.04	0.00	1.59	1.21	3.58	2.92				2.89	5.66	27.90	0.00
Total recalc.			99.52	99.22	100.03	99.76	98.25	100.05				99.51	99.59	98.17	99.53
Si	0.984	0.996	1.895	1.946	1.903	1.892			0.982	1.001	1.941	1.816	0.001	0.000	2.325
Ti			0.000	0.002	0.003	0.215	0.011	0.011			0.003	0.057	1.890	0.531	
Al			0.097	0.124	0.193	0.215	12.809	13.082			0.130	0.241	0.004	0.124	1.664
Cr	0.001	0.001	0.016	0.006	0.023	0.027	2.553	2.431		0.001	0.007			0.037	
Fe^{3+}			0.105	0.000	0.044	0.034	0.620	0.464			0.000	0.084	0.207	0.776	0.000
Fe^{2+}	0.209	0.191	0.053	0.178	0.046	0.049	1.645	1.791	0.303	0.184	0.173	0.208	1.445	1.337	0.022
Mn	0.004	0.003	0.004	0.006	0.003	0.002	0.016	0.020	0.005	0.003	0.005	0.009	0.034	0.018	
Mg	1.807	1.804	1.787	1.712	0.874	0.856	6.279	6.151	1.725	1.798	1.708	0.624	0.395	0.175	
Ca	0.003	0.003	0.030	0.015	0.831	0.842	0.002	0.000	0.002	0.003	0.020	0.856	0.012	0.001	0.679
Na			0.008	0.007	0.077	0.073	0.004	0.000				0.077			0.294
K															0.007
Ni	0.008	0.006	0.003	0.003	0.001	0.002	0.061	0.050	0.007	0.008	0.004		0.004	0.000	
Mg#			97.1	90.6	95.0	94.6	79.2	77.4			90.8	75.0			
Cr#							17.9	15.7							
Usp (%)														59.0	
Fo	89.4	90.3							84.9	90.6					
Fa	10.6	9.7							15.1	9.4					
Wo			1.6	0.9	47.5	48.2					1.0	45.7			
En			95.6	91.2	49.9	49.0					89.9	40.8			
Fs			2.8	7.8	2.6	2.8					9.1	13.5			
An															69.2
Ab															30.0
Or															0.7

4. RESULTS

4.1. Petrography

4.1.1. The host basalt

The host rock (BL) is an alkaline basalt (D.I. ≈ 25; normative nepheline ≈ 7 %), with porphyritic texture containing abundant (30 % vol.) euhedral phenocrysts of olivine (0.7-3 mm), clinopyroxene (1-2 mm), spinel and Ti-magnetite in a groundmass of lath-shaped crystals of clinopyroxene (< 0.05 mm), plagioclase microlites (0.01-0.05 mm) and a heterogeneous glass. The basalt also contains olivine, and angular and fractured orthpyroxene xenocrysts with well-developed undulose extinction.

4.1.2. The xenoliths

Lherzolites display a protogranular texture (terminology

Table 2: Chemical composition of representative minerals of the lherzolite and the host-basalt from Liri.

	Liri	Kapsiki Plateau	Mt Cameroon
Sample	BL	2X	C10J
SiO_2 (wt %)	43.99	42.87	45.00
TiO_2	2.86	2.74	2.27
Al_2O_3	12.55	11.35	8.43
FeO*	11.47	12.19	11.07
MnO	0.17	0.17	0.18
MgO	13.11	15.13	14.46
CaO	10.07	10.16	14.57
Na_2O	3.07	2.72	1.26
K_2O	0.81	1.06	0.59
P_2O_5	0.58	0.83	0.32
L.O.I.	1.18	0.20	1.87
Total	99.84	99.62	100.02
Ne	7.31	15.80	2.88
D.I.	24.57	21.92	11.71
Mg#	79.4	80.1	80.3
Rb (ppm)	22.7	22.0	14.3
Sr	732	1105	473
Cs	0.39	0.00	0.27
Ba	345	360	205
V	223	105	235
Cr	669	1101	1304
Co	53	62	57
Ni	361	0	279
Cu	50	105	55
Zn	127	92	88
Y	22.22	22.00	18.30
Zr	250.8	163	183
Nb	53.0	52.0	39.0
Hf	5.49		4.45
Ta	3.89		2.88
Th	4.31		3.26
U	1.19		0.88
La	38.2	35.5	32.7
Ce	77.7	85.0	70.0
Pr	9.49		8.70
Nd	38.8	38.3	35.1
Sm	7.91	8.30	6.80
Eu	2.60	2.67	2.10
Gd	6.68	7.70	5.51
Tb	0.93		0.76
Dy	4.76	4.40	3.97
Yb	1.56	1.23	1.37
Lu	0.22	0.22	0.19

after Mercier and Nicolas, 1975) and have a modal composition comprising olivine: 50-60 %, orthopyroxene: 20-25 %, clinopyroxene: 10-16 %, spinel: 2-4 %. Olivine is colourless and often contains deformation lamellae. It is generally coarse-grained (3-6 mm in diameter) with curved joints and is surrounded by subhedral clinopyroxene crystals with well-developed kink bands. Small polygonal olivine grains (down to 0.1 mm or less in diameter) are present and represent recrystallized olivine grains. Orthopyroxene is usually colourless, but occasionally with a brown tint. Unmixing of clinopyroxene in orthopyroxene is uncommon. Cleavage traces are commonly visible. Clinopyroxene (2-5 mm) is colourless to brown grey, and occurs as interstitial crystals between olivine and orthopyroxene crystals, displaying well-developed undulose extinction. Spinel occurs as interstitial or vermicular crystals (20-30 m), sometimes in grains (3-4 mm long) concentrated in distinct planes in the xenoliths.

4.2. Mineral chemistry

Lherzolite olivine has Fo contents between 89 and 91. It is homogeneous and shows very similar composition in different xenoliths samples. There is no chemical distinction between porphyroclastic olivine and the polygonal recrystallized varieties; a feature also observed by Temdjim (2005) in garnet lherzolites from the Adamawa. MgO and NiO (0.30-0.44 %) contents are similar to those of xenocrysts from the host basalt (Fo_{88-92}; 0.13-0.26 %). Mg-rich olivine phenocrysts are homogeneous and show very similar compositions in different samples of the host basalt. They are unzoned but sometimes have cores richer in Mg (Fo_{85-75}) than rims (Fo_{72}).

Lherzolite orthopyroxene is Al-rich enstatite (En_{89-92}). As in the case of coexisting olivine, the orthopyroxene has very constant composition from grain to grain as well as from xenolith to xenolith. Rounded and fracturated Al-rich enstatite (En93; Mg# 94) xenocrysts are present.

Clinopyroxene from lherzolite xenoliths is Al and Cr-rich diopside ($Wo_{45-48}En_{46-49}Fs_{9-3}$). Like the coexisting enstatite, the diopside to show minor variations in Al content. The average Al content in Liri lherzolite diopside is 0.71 %, which is twice the amount present in the coexisting enstatite. The clinopyroxene contains 0.4 to 2.0 % Fe_2O_3 averaging 1.2 %. When considering calculated pyroxene end-member proportions special attention is drawn to the contents of jadeite, Ca-Ti-tschermak's molecule and Ca-tschermak's molecule because of the pressure and temperature dependencies of these components. The small compositional range of the lherzolite diopside is reflected in the fact that the end-member proportions show only 11.9 mole percent, and jadeite + Ca-tschermak's molecule constitute 17.0 to 20.1 mol. %, while the amount of

Ca-Ti-tschermak's molecule are low (1.7 mol. % on average). The host basalt contains phenocrysts of diopside ($Wo_{45-47}En_{43-38}Fs_{12-15}$) with Mg# values and TiO_2 of 77-78 and 1.3-2.8 %, respectively.

Spinel from the lherzolite xenoliths is spinel sensu strictu in the terminology of Deer et al. (1975): ($Mg > Fe^{2+}$; $Al > Cr$) with Cr (Cr# = 14-17 with Cr# = Cr x 100/(Cr+Al)) and Mg (Mg# 79-82) contents similar to those of spinel from Nyos (Nana et al., 1998 ; Temdjim, 2005), Dibi (Girod et al., 1984) and Barombi and Enep (Lee et al., 1996). A certain variation in Al and Cr contents of individual spinels gives rise to a range of Cr#.

Titanomagnetite ($53 < Usp \% < 62$) and ilmenite ($TiO_2 \approx 52 \%$) from the host basalt have similar compositions to those of basalts from Kapsiki Plateau (Ngounouno et al., 2000). Equilibrium Fe-Ti oxide temperatures are between 980 and 1000°C (± 20°C) and corresponding oxygen fugacities of 10-10 (± 0.5 x 10-10) atmospheres according to Spencer and Lindsley (1981).

Plagioclase microlites from the host basalt are Ca-rich (An_{68-53}).

The above composition of various phases in the lherzolites confirms that the Liri lherzolites are typical members of the Cameroon Hot Line lherzolite xenolith suite (e.g. Lee et al., 1996; Nana et al., 1998; Princivalle et al., 2000 ; Caldeira and Munha, 2002, Déruelle et al., 1991, Teitchou et al., 2007) and of the Adamawa Plateau (Temdjim, 2005).

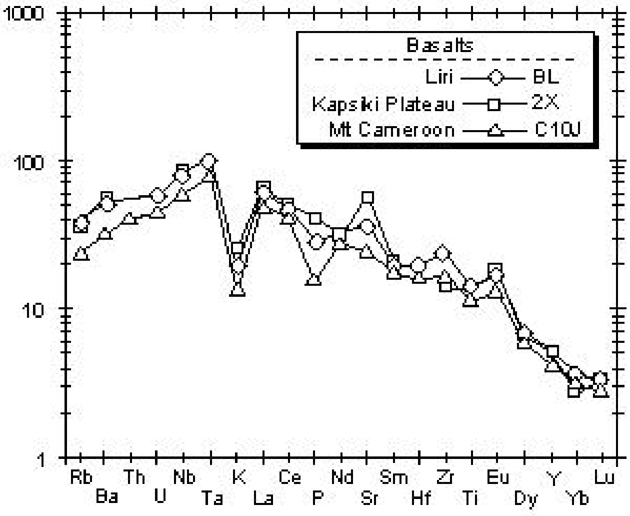

Fig. 3: Multielement spidergram of the host-basalts from Liri (BL). Basalt from Kapsiki Plateau (2X) and Mount Cameroon (C10J) are used for comparison. (normalizing values from McDonough and Sun (1995).

4.3. Geochemistry

The host basalt (BL) displays primitive characteristics (Mg# 79) with high Cr (669 ppm) and Ni (361 ppm) contents (Table 2). In primitive mantle normalized spidergrams, the host basalt and the less evolved basalts of Kapsiki Plateau and Mt Cameroon have similar patterns (Fig. 3). These are characterized by negative Rb and K and positive Zr anomalies, and have high $(La/Yb)N \approx 17$ and $(La/Sm)_N \approx 3$. The host basalt spectra are similar to those of the Cameroon Hot Line basalts (e.g. Déruelle et al., 2007).

5. DISCUSSION

The triple-point junctions (V app. 120°) seen between the silicate phases suggest that a certain degree of intergrain adjustment possibly annealing, has taken place (Vernon, 1970). The protogranular texture, undulose extinction of olivine and clinopyroxene and local recrystallization suggest that the studied xenoliths were deformed after they crystallized. In addition, lherzolites are crosscut by a thin basaltic vein. These observations suggest that it is highly unlikely that the xenoliths are cognate to their host-basalts. Also, there is no trace of plagioclase, garnet, or accessory hydrated minerals (amphibole, phlogopite, and apatite) in the mode of the xenolith.

5.1. Exchange reactions and equilibrium state

Elements are not randomly distributed between the four mineral phases (ol, opx, cpx, and sp) of the lherzolite xenoliths from Liri. In fact, their distribution is governed by a set of exchange and transfer reactions rules based on thermodynamic equilibrium conditions (Mercier and Bertrand, 1984). Here, we should review some of these reactions which must later allow to characterize the chemical composition of the upper mantle beneath the Liri region and to test the equilibrium state between these mineral phases.

In the case of the Liri peridotites, olivine and orthopyroxene constitute more than 70-90 vol.% of the rock, and their compositions very closely approach compositions of the $FeO-MgO-SiO_2$ (FMS) system. We could then characterize the chemical variation of Fe/Mg systems using the olivine/orthopyroxene pair. According to Matsui and Nishizawa (1974), the Fe-Mg exchange between olivine and orthopyroxene can be described allowing behaviour of a monosite, ideal solution for these two phases at high temperatures (> 1000°C). We must then use the following reaction to express this exchange:

$$\underset{\text{Fo (ol)}}{Mg_2SiO_4} + \underset{\text{Fs (opx)}}{Fe_2Si_2O_6} <==> \underset{\text{En (opx)}}{Mg_2Si_2O_6} + \underset{\text{Fa (ol)}}{Fe_2SiO_4}$$

The partition coefficient is expressed as follows:
$K_D = ((X_{Fe})_{ol} * (X_{Mg})_{opx} / ((X_{Mg})_{ol} * (X_{Fe})_{opx}$

In application to natural system and considering that Fe/Mg exchange is limited to octahedral sites (not occupied by Ca, Na, Cr and Al), the concentrations corresponding to the FMS-system can be estimated as:
$(X_{Mg})_{ol} = (Mg/Mg + Fe^{2+})_{ol}$ $(X_{Fe})_{ol} = 1 - (X_{Mg})_{ol}$
$(X_{Mg})_{opx} = (Mg/Mg + Fe^{2+})_{opx}$ $(X_{Fe})_{opx} = 1 - (X_{Mg})_{opx}$

Assuming the Mg/(Mg + Fe) ratio of olivine and orthopyroxene of peridotites, the Mg/(Mg + Fe)ol versus $(Mg/(Mg + Fe)_{opx}$ diagram (Fig. 4) is constructed and the partition coefficient is determined and compared to a theoretical model. Figure 4 shows an excellent correlation between olivine and orthopyroxene indicating partition coefficients higher than 1, except for peridotites from Ngaoundéré and Dibi (Dautria and Girod, 1986; Lee et al., 1996) for which the average partition coefficient is 0.94. The small compositional range of the Fo content of olivine is in the same general range of the mantle rocks (90-92; Sato et al., 1991).

Due to the fact that Al and Cr contents are concentrated in spinel, but are also present in pyroxene in small amounts, the second exchange reaction is:

$(Mg, Fe)_3Al(AlSi_3O_{12})$ + ½ $(Mg, Fe)Cr_2O_4$
(opx) (sp)

<==> $(Mg, Fe)_3Cr(AlSi_3O_{12})$ + ½ $(Mg, Fe)A_{l2}O_4$
(opx) (sp)

In fact, Ganguly and Ghose (1979) pointed out by experimentally measuring the interatomic lattice in pyroxene, that Al occupies both tetrahedral and octahedral sites while Cr is restricted to the octahedral sites. They concluded that the Cr-Al exchange is limited to octahedral sites. To maintain the electroneutrality of the phase, the presence of Na in the pyroxene needs an equivalent amount of trivalent cations (Al, Cr and Fe^{3+}). The content of these three elements is relatively constant in the presence of a given Al-rich phase for peridotites derived from the upper mantle (Mercier, 1980; Bertrand et al., 1987). In our case, for the spinel facies, the amount of ferric iron in the pyroxenes (Table 1) is very low and any significant value could be calculated from electron microprobe results. In summary, to express Al-Cr exchange between orthopyroxene and spinel, we should calculate the amount of Al^{VI} (none associated with Na): (Al - Cr - Na)/2 and Al^{IV} = (Al + Cr - Na)/2). The (Cr/Cr + Al)sp versus $(Cr/Al^{IV})_{opx}$ diagram (Fig. 5) is used in order to describe in appropriate manner this exchange. The pattern observed implies a non-ideal spinel composition with respect to the Y-site for a Cr-Al substitution. This agrees with

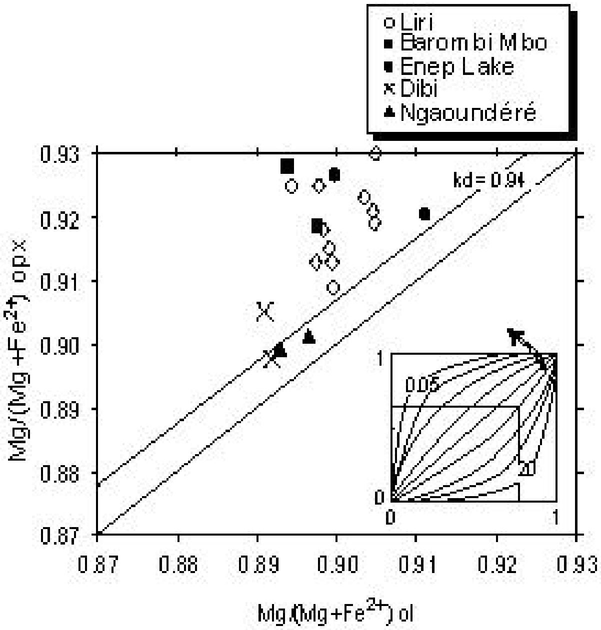

Fig. 4: Fe-Mg exchange diagram between olivine and orthopyroxene. The inset is calculated by a model of fictive ideal solution assuming octahedral sites for the two phases.

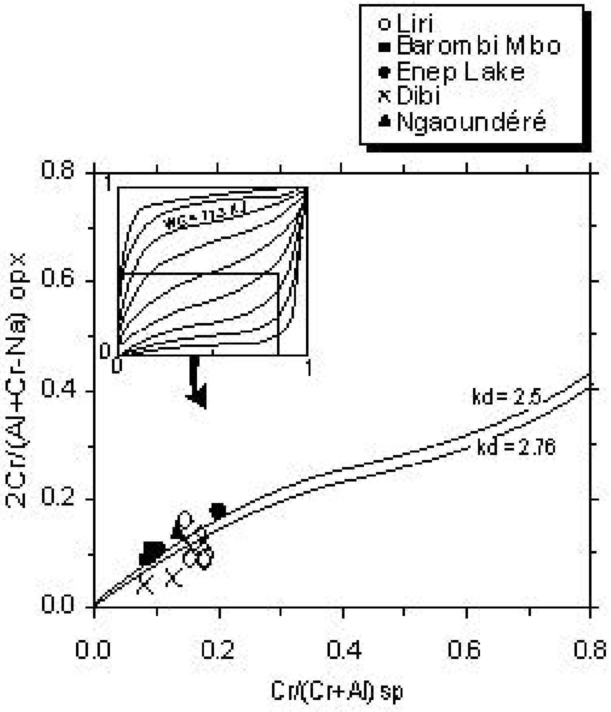

Fig. 5: Cr-Al exchange diagram between spinel and orthopyroxene. The model of regular solution has been calculated at 900 °C (inset) with an excess energy of 11.3 kj (Webb and wood, 1986) for Cr/Al interactions in Y-sites of the spinel.

experimental and theoretical data showing that a simple model of regular solution will be convenient to describe this Al-Cr partitioning between spinel and orthopyroxene.

Note that:

$X_2 = X_1/(X_1 + K(1 - X_1) \exp(W_G(2X_1 - 1)/RT$ for T fixed with; where

$X_1 = (Cr/(Cr + Al))_{sp}$ and

$X_2 = (2Cr/(Al + Cr - Na))_{opx}$, WG (2X1 - 1)

RT being excess of energy with a value of 11.3 kJ for the parameter of Margules WG, according to Webb and Wood (1986). This expression allows calculating the theoretical Al - Cr partition between spinel and orthopyroxene which is represented by asymmetrical curves contrasting with those shown in Figure 4. The majority of representative compositions plot on the curve corresponding to an equilibrium constant of 2.5.

The Al-Cr exchange between the two pyroxenes is well described by a model of ideal solution using the $(Cr/{}^{IV}Al)_{cpx}/(Cr/{}^{IV}Al)_{opx}$ pair and an equilibrium constant written as follows: $K_D = (X_{Al})_{opx}(X_{Cr})_{opx}/(X_{Cr})_{opx}(X_{Al})_{opx}$ with $(X_{Cr})_{opx} = 2Cr/(Al + Cr ? Na)$ and $(X_{Al})_{opx} = 1 - (2Cr/(Cr + Al - Na))$. The equilibrium constant is significantly different from unity and is about 3.3 for peridotites from Liri (Fig. 6). Cr and Al contents of clinopyroxene are twice the amount of those of orthopyroxene. The observed correlation confirms what was seen in the previous diagrams (Figs 3, 4): lherzolite samples from Liri as well as those from the Barombi Mbo, Lake Enep, and Ngaoundéré and Dibi attest a good internal equilibrium, and quite represent a normal mantle.

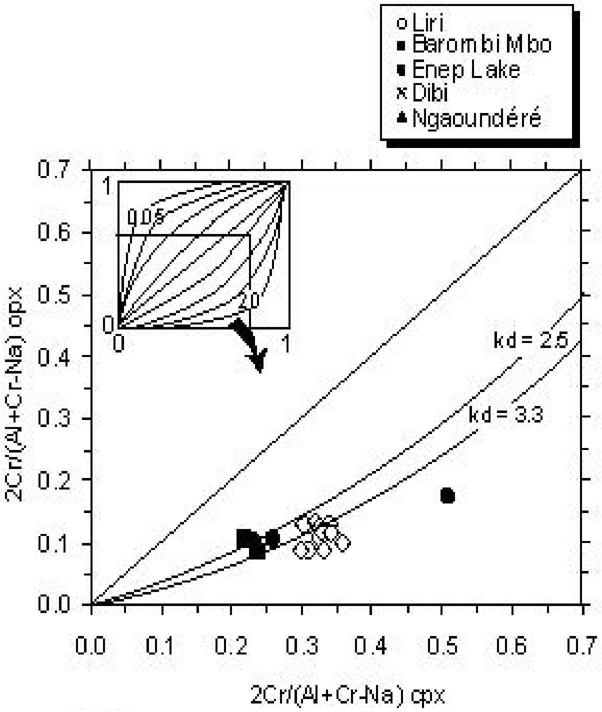

Fig. 6: Cr-Al exchange diagram between the two pyroxenes. Only Cr and Al in octahedral sites have been taken into account in the exchange.

Due to the effects of interactions of Fe and Mg cations in the X-sites and Al and Cr in the Y-sites, spinel could not be considered as a monosite ideal solution for the Fe-Mg substitution. These interactions can be described by the following reaction:

$FeAl_2O_4 + MgCr_2O_4 <===> FeCr_2O_4 + MgAl_2O_4$

This is well described using the $(Mg/Mg+Fe^{2+})_{sp}$ versus $(Cr/Cr+Al)_{sp}$ diagram (Fig. 7). As spinel is richer in Cr than other minerals, the $Cr\#_{sp}$ reflects the system and controls the $Mg\#_{sp}$. For comparison, the composition of lherzolites from Liri, Barombi Mbo, Lake Enep, and Ngaoundéré and Dibi, and ophiolitic peridotites (Cabanes and Mercier, 1988) are also reported on Figure 7. The investigated lherzolites and those from other parts of the Cameroon Hot Line, and Ngaoundéré and Dibi (Dautria and Girod, 1986; Lee et al., 1996) are clearly distinct in chemistry and are located above the field of ophiolites (Cabanes and Mercier, 1988), in the domain of spinel peridotites derived from lithospheric mantle (Conticelli and

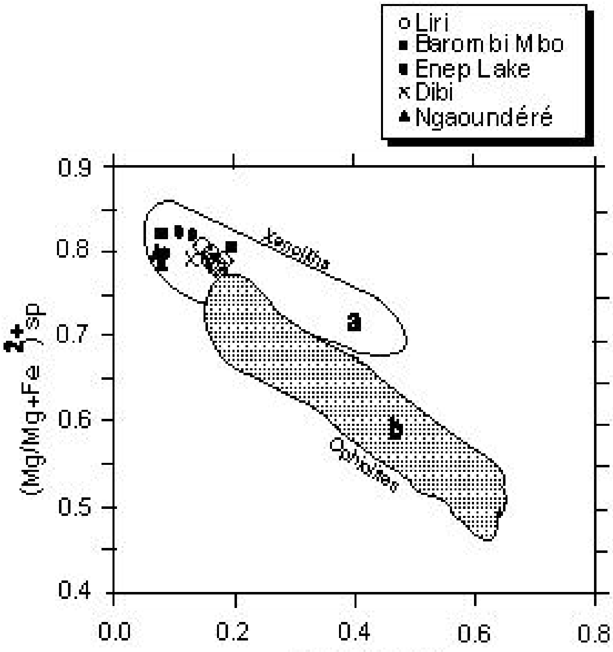

Fig. 7: Fig. 7: Mg-Cr diagram for spinel.

a: Domain of ultrabasic xenoliths (lherzolites and harzburgites) in basaltic lavas (after Conticelli and Piccerillo, 1990).

b: Domain of ultrabasic xenoliths in ophiolites (Cabanes and Mercier, 1988b).

Piccerillo, 1990). The distinct chemical differences between lherzolite xenoliths and ophiolites were explained by kinetics of this exchange reaction (Cabanes and Mercier, 1988).

5.2. Geothermometry and geobarometry of spinel lherzolite xenoliths

We evaluated three different geothermometers for the Liri lherzolite xenoliths. Equilibrium temperatures of 1050-1100°C are estimated using the olivine/spinel geothermometer of Fabriès (1979), using crystal cores analyses. As the Fo content of olivine from lherzolites is obviously high, (between 89 and 91 %) and spinel and orthopyroxene contain very small amounts of Fe^{3+}, (which could only have insignificant effect on temperature calculations), it seems reasonable to use this geothermometer. Equilibrium temperature estimates fall between 1130 and 1190°C, using Bertrand and Mercier's (1985) two-pyroxene geothermometer. Applying the geothermometer of Bertrand et al. (1987), based on the solubility of Al_2O_3 in clinopyroxene and orthopyroxene, the temperature expression calibrated at 1.5 GPa in a natural spinel lherzolite system, gives the equilibrium temperatures of individual Liri lherzolite xenoliths as 1158-1166°C. In conclusion, the overall impression is that the equilibrium temperatures of spinel lherzolite xenoliths from Liri lie in the same general range as equilibrium temperatures of a number of other lherzolite xenoliths along the Cameroon Hot Line, and Ngaoundéré and Dibi (Dautria and Girod, 1986; Lee et al., 1996). More specifically, Liri lherzolite equilibrium temperatures lie 200°C below the dry peridotite solidus at 1.5 GPa (Wyllie, 1970), but nearly 300°C above the water saturated peridotite solidus at the same pressure (Mysen and Boettcher, 1975).

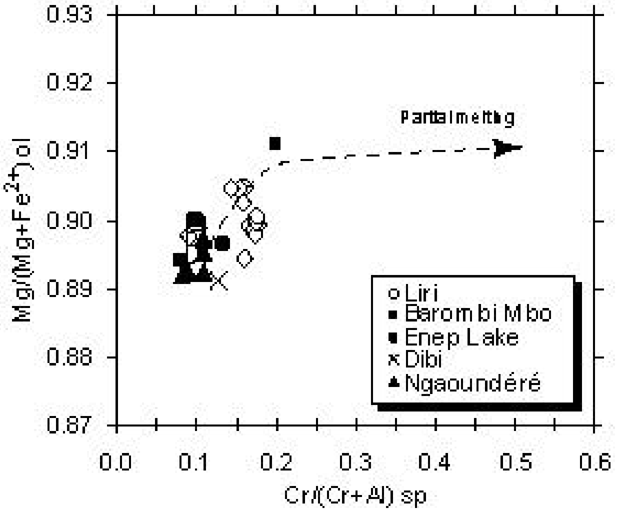

Fig. 8: Mg# versus Cr# diagram illustrating the compositional evolution of the peridotite system strongly depending on partial melting.

The lack of plagioclase or garnet in lherzolites and the fact that the lherzolite xenoliths have reached a high degree of internal chemical equilibrium, indicate that equilibration took place at pressures ranging between 1.4 and 2.3 GPa (55-80 kms). Liri xenoliths have probably been sampled by the host-basalt in the upper mantle. At depths of 60-80 kms, the calculated temperatures are about 200°C above those of the oceanic geotherm of Clarke and Ringwood (1964). It seems noteworthy that lherzolite xenoliths along the Cameroon Hot Line likewise have equilibrium temperatures about 200°C above the oceanic geotherm (Lee et al., 1996).

5.3. Origin of spinel lherzolite xenoliths

Lherzolite xenoliths, characterized by the presence of Cr-diopside, in alkaline basaltic rocks represent portions of the earth's upper mantle (cf. Green and Ringwood, 1967) or represent cumulates crystallized from their host rocks (O'Hara and Mercy, 1963; O'Hara, 1968, 1970). How do these two competing models compare in the light of mineral chemistry evidence from the Liri lherzolite xenoliths?

The composition of olivine and spinel is strongly dependent on the degree of melting, a feature characterized firstly by a regular increase of $(Mg\#)_{ol}$, $(Mg\#)_{sp}$ and $(Cr\#)_{sp}$ values and secondly by the fact that these values remain nearly constant through the melting process (Mysen and Kushiro, 1977). As Cr is a refractory element, it is enriched in the residue. The overall representative analyses are grouped around a restricted range (Fo89-91) (Fig. 8). Based on these data, the xenoliths from Liri represent a residual sequence issued from partial melting of a mantle source.

Experiments have shown that the composition of solid solutions, such as olivine, is very sensitive to temperature changes, and olivine could therefore evolve towards refractory compositions during the partial melting. So, an extraction of the melt could leave a residue depleted in highly incompatible elements (e.g. Na, Al, K, and Ti) and enriched in Cr and Ni relative to the most primitive mantle (Hart and Zindler, 1985). Na and Ti contents decrease with $(Cr\#)_{sp}$ (Fig. 9), a pattern similar to that previously observed in the precedent figures. But, while the chemical evolution of Ti contents is well explained by a melting process, the highly incompatible behaviour of Na is more complicated, with many analyses plotting above the region predicted for primitive mantle. These discrepancies could certainly imply metasomatic effect.

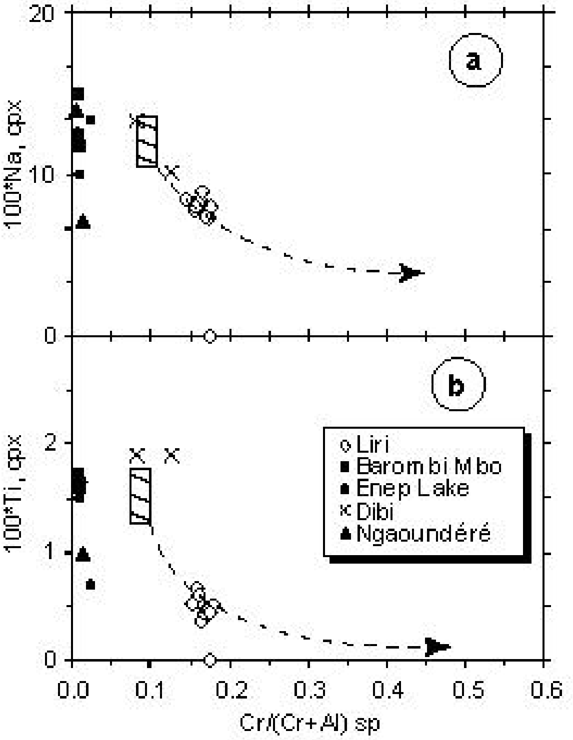

Fig. 9: Correlation between incompatible elements and the degree of partial melting in clinopyroxene and spinel.
a: (100*Na)cpx versus (Cr/Cr+Al)sp.
b: (100*Ti)cpx versus (Cr/Cr + Al)sp.

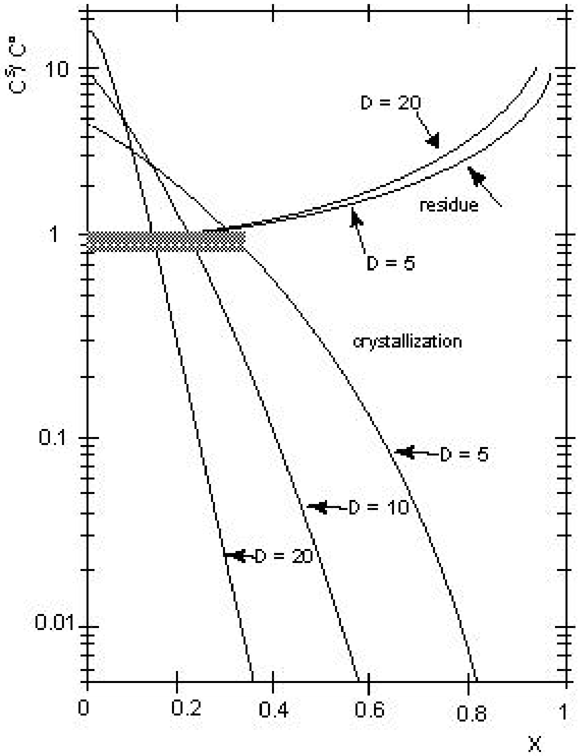

Fig. 10: Variation of the theoretical $C^s/C°$ ratio during the partial melting and fractional crystallization for different partition coefficients. X is the degree of melting or crystallization. The grey part indicates the variation of Ni contents for the studied xenoliths

The range of Ni contents of olivine of lherzolites from Liri confirms that they are residue of melting. This is illustrated in Figure 10 and can be deduced from the non-modal batch melting equation of Shaw (1970): $CNi^s/CNi^0 = D_{Ni}^{s/l}/(D_{Ni}^{s/l}(1 - F) + F)$ where F is the degree of melting; C_{Ni}^s and C_{Ni}^0 are the concentration of Ni in the residue and the source; $D_{Ni}^{s/l}$ is the bulk distribution coefficient of Ni in the initial assemblage and for the minerals entering into the liquid, respectively.

The fact that Ni behaves as a highly compatible element, i.e. $D_{Ni}^{s/l} >> 1$ allows us to assume that $D_{Ni}^{s/l} >> F$ (e.g. Hart and Davis, 1978) and simplify the partial melting expression as follows: $C_{Ni}^s/C_{Ni}^0 = 1/(1 - F)$. The degree of melting can be accurately estimated taking into account this approach and also the high proportion of olivine.

The Ni content is very high (2190-3331 ppm) in olivine, while it is only 130-936 ppm in clinopyroxene and 285-1181 ppm in orthopyroxene. For spinel, the Ni content is somewhat similar to that of olivine, but spinel is a minor mineral phase (< 5 vol. %) and so its role is still insignificant. The Ni content of olivine could represent the maximum content of the bulk-rock compositions. Assuming that the initial concentration of Ni in the primitive mantle is $C_{Ni}0 = 2108$ ppm (Jagoutz et al., 1979), the Ni contents of the Liri samples were plotted in Fig. 10. It can be observed that for an interval degree of melting or crystallization, the range of Ni content resulting from fractional crystallization is larger than that generated from the residue. For example, the C^s/C^o ratio varies from 5 to 1.2 with $D^{s/l} = 5$ and requires 30 % of crystallization. This is particularly obvious for the highest $D^{s/l}$ values. On the other hand, under similar conditions, the C^s/C^o ratio changes from 1 to 1.33 during partial melting. To summarize, it appears that high content of Ni (2190-3331 ppm) in olivine suggests that xenoliths from Liri could derive from a low degree of melting (< 30 %) of a relatively homogeneous mantle source.

There is thus no need to appeal to a cumulate crystallized rocks model of the kind proposed by O'Hara and Mercy (1963), O'Hara (1968, 1970). Rather, the model of Green and Ringwood (1967) for portions of the earth's upper mantle appears appropriate for the origin of the Liri lherzolite xenoliths.

5.4. Origin of the host basalt

The host basalt (BL) represents the most primitive lava erupted in the Liri region. It has high MgO (13.0 wt %), Ni (361 ppm) and Cr (669 ppm) and high *mg*-number (79), consistent with a derivation from partial melting of a peridotite mantle source. Xenocrysts of olivine (Fo_{88-92}) and orthopyroxene (Mg# 94) have been found in this basalt. They may be individual crystals resulting from the disaggregation of peridotite xenoliths. The modal abundances of these xenocrysts is very low (< 0.1 vol. % for orthopyroxene and < 0.2 vol. % for olivine) so that the chemistry of the host basalt is not significantly affected by their occurrence. The parental magma of the Liri basalts could have incorporated accidental fragments of a spinel-peridotite during their rise through the lithosphere. These rising magmas may have accumulated in reservoirs at the crust-mantle boundary beneath the Liri shield, as suggested by the presence of orthopyroxene and olivine xenocrysts in the basalt (BL) which implies a minimum depth of $\approx$ 30-50 km, estimated (e.g. Walter and Presnall, 1994) from the stability field of spinel peridotite at liquidus temperature (1300-1400°C). This depth is consistent with the crust-mantle boundary locally estimated at 37-44 km from seismic refraction studies (Dorbath et al., 1986).

6. CONCLUSION

The ultramafic xenoliths exhumed by alkali basalts from Liri South of Kapsiki Plateau are classical spinel lherzolites. Major and trace elements and mineral chemistry indicate that these lherzolites are residues of partial melting of an initial mantle with a degree of melting lower than 30 %. The spinel lherzolites show internal chemical homogeneity, and their mineral chemistries suggest equilibrium conditions of 1050-1200°C and 1.4-2.3 GPa. Major and trace element contents of the investigated host basalt suggest derivation from the earth's upper mantle by a small degree of partial melting.

REFERENCES

Bertrand P. Mercier J.C.C. (1985). The mutual solubility of coexisting ortho-and clinopyroxene: toward an obsolute geothermometer for natural system? *Earth and Planetary Science Letters* 77, 109-122.

Bertrand. P., Sotin C., Gaulier J.M., Mercier J.C.C. (1987). La solubilité de l'aluminium dans l'orthopyroxène. Inversion globale des données expérimentales de $MgO-Al_2O_3-SiO_2$. *Bulletin Société Géologique de France* 821-832.

Cabanes N., Mercier J.C.C. (1988). Insight into the upper mantle beneath an active extensional zone: the spinel-peridotite xenoliths from San Quintin (Baja California, Mexico). *Contributions to Mineralogy and Petrology* 100, 374-382.

Caldeira R., Munha J.M. (2002). Petrology of ultramafic nodules from Sao Tomé Island, Cameroon Volcanic Line (oceanic sector). *Journal of African Earth of Sciences* 34, 231-246.

Carignan J., Hild P., Mévelle G., Morel J., Yeghicheyan D. (2001). Routine analyses of trace elements in geological samples using flow injection and low pressure on-line liquid chromatography couples to ICP-MS: a study of geochemical reference materials BR, DR-N, UB-N, AN-G and GH, *Geostandards Newsletters* 25, 187-198.

Clarke S.P., Ringwood A.E. (1964). Density distribution and constitution of the mantle. *Review of Geophysics* 2, 35-88.

Conticelli S., Piccerillo A. (1990) Petrological significance of high-pressure ultramafic xenoliths from ultrapotassic rocks of central Italy. *Lithos* 24, 305-322

Dautria J.M., Girod M. (1986). Les enclaves de lherzolite à spinelle et plagioclase du volcan de Dibi (Adamaoua, Cameroun) : des témoins du manteau anormal. *Bulletin de Minéralogie* 109, 275-286.

Deer W. A., Howie R. A., Zussman J. (1975). An introduction to the rock-forming minerals. Longman.

Déruelle B., Moreau C., Nkoumbou C., Kambou R., Lissom J., Njongfang E., Ghogomu R.T., Nono. (1991). The Cameroon Line: a review, in: Kampunzu A.B., Lubala R.T. (Eds), Magmatism in Extensinal Structural Settings. The Phanerozoic African Plate. *Springer-Verlag,* Heidelberg pp. 274-327.

Déruelle B., Ngounouno I., Demaiffe D. (2007). The 'Cameroon Hot Line' (CHL): A unique example of active alkaline intraplate structure in both oceanic and continental lithospheres, *Comptes Rendus Geoscience* 339, 589-600.

Dorbath C., Dorbath L., Fairhead J.D., Stuart G.W. (1986). A teleseismic delay time study across the Central African Shear Zone in the Adamawa region of Cameroon, West Africa. Geophys. *Journal of the Royal Astronomy Society* 86, 751-766.

Droop G.T.R. (1987). A general equation for estimating Fe3+ concentrations in ferromagnesian silicates and oxides from microprobre analyses, using stochiometric criteria. *Mineralogical Magazine* 51, 431-435.

Dumort J.-C., Péronne Y. (1966). Carte Géologique de Reconnaissance à l'échelle du 1/500 000, République Fédérale Cameroun, feuille Maroua. BRGM et Direction Mines et Géologie Cameroun, avec notice explicative, 50pp.

Dunlop H.M. (1983). Strontium isotope geochemistry and potassium-argon studies on volcanic rocks from the Cameroon line, West Africa. PhD thesis, Univrsity of Edinburgh, 347p.

Fabriès J. (1979). Spinel-olivine geothermometry in peridotites from ultramafic complexes, *Contributions to Mineralogy and Petrology* 69, 329-336.

Girod M., Dautria J.-M., Balle, Soba D. (1984). Estimation de la profondeur du manteau du Moho sous le massif volcanique de l'Adamaoua (Cameroun) à partir de l'étude d'enclaves de lherzolite. *Comptes Rendus de l'Académie des Sciences* Paris 298, 699-704.

Green D.H., Ringwood A.E. (1967). The genesis of basaltic magmas. *Contributions to Mineralogy and Petrology* 15, 103-190.

Green D.H., Ringwood A.E. (1970). Mineralogy of peridotitic compositions under upper mantle conditions. *Physical Earth and Planetary Interiors* 3, 359.

Hart S.R., Davis K.E. (1978). Nickel Partitioning between Olivine and Silicate Melt. *Earth and Planetary Science Letters* 40(2), 203-219.

Jagoutz E., Palme H., Baddenhausen H., Blum K., Cendales M., Dreibus G., Spettel B., Lorenz V., Wanke H. (1979). The abundances of major, minor and trace elemnts in the earth's mantle as derived from primitive ultramafic nodules. Proceedings of the 10th Lunar Planetry Science Conference, pp. 2031-2050.

Lee D.C., Halliday A.N., Davies G.R., Essene E.J., Fitton G.J. Temdjim R. (1996). Melt enrichment of shallow depleted mantle: a detailed petrological, trace element and isotopic study of mantle-derived xenoliths and megacrysts from the Cameroon Line. *Journal of Petrology* 37, 415-441.

Matsui Y., Nishizawa O. (1974). Iron (II). Magnesium exchange equilibrium between olivine and calcium-free over a température range 800°C to 1300°C. *Bulletin Société Française de Minéralogie et Cristallographie* 97, 122-130.

Mercier J.C., Nicolas A. (1975). Textures and fabrics of upper mantle peridotites as illustrated by xenoliths from basalts. *Journal of Petrology* 16, 454-487.

Mercier J.C.C. (1980). Single-pyroxene thermobarometry. *Tectonophysics* 70, 1-37.

Mercier J.C.C., Bertrand P. (1984). Thermobarométrie pyroxènique: quelques méthodes basées sur les réactions de transfert. In "Thermométrie et Barométrie géologiques ", V. Gabis et M. Lagache Eds. Société Française de Minéralogie et Cristallographie, Paris, 237-280.

Morimoto N., Fabriès J., Ferguson A.K., Ginzburg I.V., Ross M., Seifert F. A., Zussman J., Aoki K., Gottardi G. (1988). Nomenclature of pyroxenes. *American Mineralogist* 73, 1123-1133.

Moreau C., Regnoult J.-M., Déruelle B., Robineau B. (1987). A new tectonic model for the Cameroon Line, Central Africa. *Tectonophysics* 13, 317-334.

Mysen B. O., Boettcher A.L. (1975). Melting of a hygrous mantle: I. Phase relations of natural peridotite at high pressures and temperatures with controlled activities of water, carbon dioxide and hydrogen. *Journal of Petrology* 16, 520-548.

Mysen B. O., Kushiro I. (1977). Compositional variations of coexisting phases with degrees of melting of peridotite in the upper mantle. *American Mineralogist* 62, 843-865.

Nana R., Nkoumbou C., Tchouankoué J.P., Tabod F. Tchoua F. (1998). Pétrologie des nodules de péridotites de Nyos (Cameroun): implications sur l'évaluation des risques volcaniques. In : Géosciences au Cameroun, J.-P. Vicat, P.Bilong (Eds), Presses Université Yaoundé I, 225-228.

Ngounouno., Déruelle B., Demaiffe D. (2000). Petrology of the bimodal Cenozoic volcanism of the Kapsiki plateau (northernmost Cameroon, Central Africa). *Journal of Volcanology and Geothermal Research* 102, 21-44.

Ngounouno I. Déruelle B. Montigny R., Demaiffe D. (2006). Les camptonites du Mont Cameroun, Cameroun, Afrique. *Comptes Rendus Geoscience* 338, 537-544.

Ngounouno I., Déruelle B. (2007). Pétrologie des xénolites de wherlites et clinopyroxénites du Mont Cameroun : évidence d'un métasomatisme mantellique. *Journal of the Cameroon Academy of Sciences* 7, 35-45.

Pouchou J.L., Pichoir F. (1991). Quantitative analysis of homogenous or stratified microvolumes applying the model "PAP". In: Electron Probre Quantitification, K.F.J.Heinrich D.E. Newbury (Eds) Plenum Press, New York, 31-75.

O'Hara M.J., Mercy E. L.P. (1963). Petrology and petrogenesis of some garnetiferious peridotites. *Trans. Royal Society of Edinburg* 65, 251-314.

O'Hara, M.J. (1968). The bearing of phase equilibria studies in synthetic and natural systems on the origin and evolution of basic and ultrabasic rocks. *Earth Science Review* 4, 69-133.

O'Hara, M.J. (1970). Upper mantle composition inferred from laboratry experiments and observations of volcanic products. *Physical Earth and Planetary Interiors* 3, 69-133.

Principalle F., Salviulo G., Marzoli., Piccirillo E.M. (2000). Clinopyroxene of spinel-peridotite mantle from lake Nji (Cameroon Volcanic Line, West Africa): crystal chemisty and petrological implications. *Contributions to Mineralogy and Petrology* 139, 503-508.

Regnoult J.-M., Déruelle B. (1983). Esquisse géologique télé-interprétative de la République unie du Cameroun au nord du 4è parallèle, 1/1 000 000. Ministère des Mines et Energie, Direction Mines et Géologie, une carte.

Sato H., Aramaki S., Kusakabe M., Hirabayashi J-I., Sano Y., Nogiri Y., Tchoua F. (1990). Geochemical difference of basalts between polygenetic and monogenetic volcanoes in the central part of the Cameroon volcanic line. *Geochemical Journal* 24, 357-370.

Shaw D.M. (1970). Trace element fractionation during anatexis. *Geochimica et Cosmochima Acta* 34, 237-243.

Spencer K.J., Lindsley D.H. (1981). A solution model for coexisting iron-titanium oxides. *American Mineralogist* 66, 1189-1201.

Stormer C.Fr. (1983). The effects of recalculation on estimates of temperature and oxygen fugacity from analyses of multicomponent iron-titanium oxides. *American Mineralogist* 68, 586-594.

Tamen J., (1998). Contribution à l'étude géologique du plateau Kapsiki (Extrême-Nord, Cameroun) : volcanologie, pétrologie et géochimie. Thèse Doctorat 3ème cycle, Université Yaoundé I, 127 pp.

Teitchou M.I., Grégoire M., Dantas C., Tchoua F.M. (2007). Le manteau supérieur à l'aplomb de la plaine de Kumba (ligne du Cameroun), d'après les enclaves de péridotites à spinelle dans les laves basaltiques, *Comptes Rendus Geoscience* 339 101-109

Temdjim R. (2005). Contribution à la connaissance du manteau supérieur du Cameroun au travers de l'étude des enclaves ultrabasiques et basiques par les volcans de Youkou (Adamaoua) et de Nyos (Ligne du Cameroun). Thèse de Doctorat d'Etat Université de Yaoundé 1, 339 p

Vernon R.H. (1970). Comparative grain-boundary studies of some basic and ultrabasic granulites. Nodules and cumulates. *Scott. Journal of Geology* 6, 337-351.

Walter M.J., Presnall D.C. (1994). Melting behavior of simplified lherzolite in the system $CaO-MgO-Al_2O_3-SiO_2-Na_2O$ from 7 to 35 kbar. Jounal of Petrology 35, 329-359.

Webb S. A., Wood B. J. (1986). Spinel-pyroxene-garnet relationships and their dependance on Cr/Al ratio. Contributions to Mineralogy and Petrology 92, 471-480.

Received: 30/08/2006

Accepted: 05/01/2008